ACS SENSORS

pubs.acs.org/acssensors

Article

CRISPR/Cas-Assisted Colorimetric Biosensor for Point-of-Use Testing for African Swine Fever Virus

Jisun Ki, Hee-Kyung Na, Sun Woo Yoon, Van Phan Le, Tae Geol Lee,* and Eun-Kyung Lim*

Cite This: *ACS Sens.* 2022, 7, 3940−3946

Read Online

ACCESS | Metrics & More | Article Recommendations | Supporting Information

ABSTRACT: African swine fever virus (ASFV) causes a highly contagious and fatal disease affecting both domesticated and wild pigs. Substandard therapies and inadequate vaccinations cause severe economic damages from pig culling and removal of infected carcasses. Therefore, there is an urgent need to develop a rapid point-of-use approach that assists in avoiding the spread of ASFV and reducing economic loss. In this study, we developed a colorimetric sensing platform based on dual enzymatic amplification that combined the clustered regularly interspaced short palindromic repeats (CRISPR)/CRISPR-associated protein 12a (Cas12a) system and the enzyme urease for accurate and sensitive detection of ASFV. The mechanism of the sensing platform involves a magnetic bead-anchored urease-conjugated single-stranded oligodeoxynucleotide (MB@urODN), which in the presence of ASFV dsDNA is cleaved by activated CRISPR/Cas12a. After magnetically separating the free urease, the presence of virus can be confirmed by measuring the colorimetric change in the solution. The advantage of this method is that it can detect the presence of virus without undergoing a complex target gene duplication process. The established method detected ASFV from three clinical specimens collected from porcine clinical tissue samples. The proposed platform is designed to provide an adequate, simple, robust, highly sensitive and selective analytical technique for rapid zoonotic disease diagnosis while eliminating the need for vast or specialized tools.

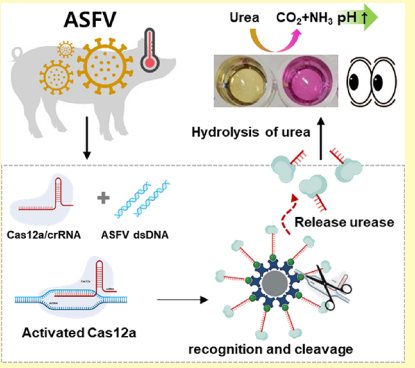

KEYWORDS: *CRISPR/Cas12a, nucleic acid detection, African swine fever virus, colorimetric, point-of-care test*

African swine fever (ASF) caused by the African swine fever virus (ASFV) is a fatal hemorrhagic disease in domestic pigs and wild boars, first identified in Kenya in 1921.[1] It has then spread throughout Eastern Europe, initially arriving in China in 2018 and spreading to most Asian countries thereafter.[2,3] Due to the lack of effective therapies and vaccinations, the spread of the disease can only be controlled by culling the infected herd and enforcing stringent quarantine protocols.[4] As a result, ASFV has caused significant socio-economic loss to the global swine industry and is designated as a notifiable disease by the World Organization for Animal Health (formerly, the Office International des Epizooties (OIE)).[5] Therefore, development of a rapid and accurate diagnostic approach is urgently required to manage this zoonotic disease and minimize its economic impact.

Among the available diagnostic methods, nucleic acid detection is the most extensively used diagnostic approach for ASF diagnosis because of its high sensitivity and specificity.[6,7] The gold standard for nucleic acid diagnosis is quantitative PCR (qPCR), which requires low sample volumes to analyze the target with high sensitivity in real time. However, despite its numerous benefits, qPCR requires costly equipment and trained operators, which restricts the processing of large numbers of samples in underprivileged settings.[8] Therefore, to overcome these limitations, several portable nucleic acid detection systems, such as high-performance isothermal amplification methods, including loop-mediated isothermal amplification (LAMP),[9,10] recombinant polymerase amplification (RPA),[11,12] and exponential amplification reaction (EXPAR) have been developed as alternatives to conventional PCR methods.[13] Numerous variants of isothermal nucleic acid amplification techniques are rapid and cost-effective molecular-based detection techniques that meet the requirements of point-of-care test (POCT) applications.[14] However, isothermal nucleic acid amplification might yield unpredictable and nonspecific amplification products, which can impact sensor specificity if a nonspecific signal is mistaken for a signal generated by the target gene.[15−17]

The clustered regularly interspaced short palindromic repeats (CRISPR)/CRISPR-associated protein 12a (Cas12a) system has broadened its applications from genomic engineering to molecular diagnostics, owing to its high sensitivity to mismatches between the target DNA and gRNA and *trans*-

Received: September 14, 2022
Accepted: November 8, 2022
Published: November 18, 2022

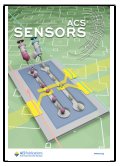

https://doi.org/10.1021/acssensors.2c02007
ACS Sens. 2022, 7, 3940−3946

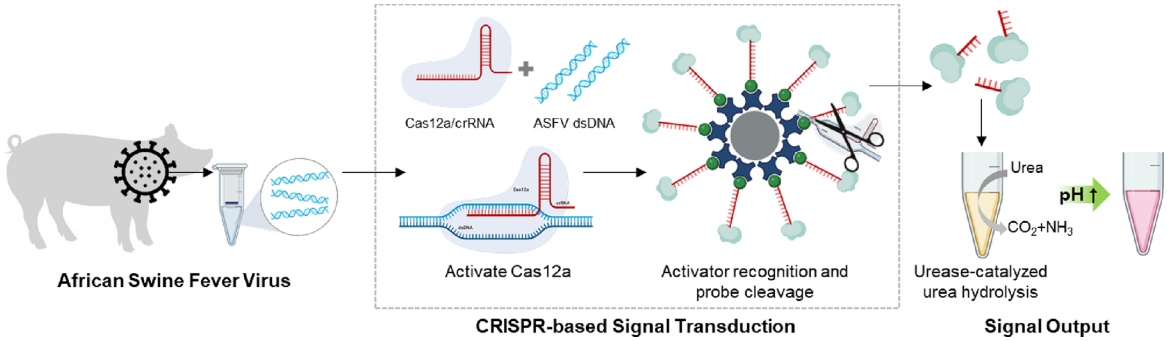

Figure 1. Schematic illustration of the CRISPR/Cas12a-based sensor array for dsDNA viral infection diagnosis using urease. In the presence of the target, crRNA/Cas12a initiates the *trans*-cleavage of the nonspecific single-stranded oligonucleotide reporter, which can be observed by a magenta color change [illustration created with BioRender.com].

cleavage mechanisms.[18−20] The *trans*-cleavage activity of the CRISPR/Cas system, activated by target DNA recognition (single-, double-stranded DNA), enables cleavage of the surrounding nontarget single-stranded DNA in the reaction system generating thousands of turnovers. Based on this property, a series of sensitive and rapid diagnostic techniques, such as DNA endonuclease-targeted CRISPR trans reporter (DETECTR), specific high-sensitivity enzymatic reporter unlocking (SHERLOCK),[21] and a one-hour low-cost multipurpose highly efficient system (HOLMES),[22] have been proposed.[23] Among these, the fluorescence output mode is the most commonly utilized approach; however, it is expensive and impractical for large-scale operations in resource-poor underprivileged areas. Therefore, there is an urgent need to develop a diagnostic method based on the CRISPR/Cas12a, which can allow the target detection with minimal dependency on experimental instruments.

Colorimetric biosensing systems have several unique characteristics, including simplicity, low cost, ease of use, and accessibility. Here, we developed a colorimetric diagnostic method, which combined the CRISPR/Cas12a target recognition system[24] with the enzyme urease-based cascade reaction-induced absorbance shift approach to develop a sensitive POCT for ASFV detection (Figure 1). This method uses Cas12a enzymes for highly sensitive nucleic acid detection of ASFV and has potential application in its early diagnosis of fatal disease in pig farms to avoid the spread of the virus. This study holds significant relevance in providing a simple and rapid viral detection diagnostic approach that utilizes the double enzyme effect without the need for amplification of the target gene. Although the sensitivity of this method might be slightly lower than those obtained in other studies, it is more effective and practical to be used in farms without requiring costly equipment or trained operators. This method has potential applications in detection of other virus and bacterial detection fields, which may assist in monitoring infectious disease pathogens and generating a rapid response plan.

2. EXPERIMENTAL SECTION

2.1. Materials and Instruments. Urease powder from *Canavalia ensiformis* (jack bean), phenol red, sulfosuccinimidyl 4-(*N*-maleimidomethyl)cyclohexane-1-carboxylate (Sulfo-SMCC), urea, sodium chloride, polysorbate 20 (Tween 20), and ethylenediaminetetraacetic acid (EDTA) were obtained from Sigma-Aldrich (St. Louis, MO, USA). Synthetic oligonucleotides used in this study, their sequences, and functions are listed in Table S1. Modified DNA oligonucleotides were purchased from Bioneer (Daejeon, Republic of Korea) and Integrated DNA Technologies (Coralville, IA, USA). M-270 streptavidin magnetic beads were obtained from Thermo Fisher Scientific Inc. (Waltham, MA, USA). Dulbecco's phosphate-buffered saline (D-PBS) (1×) was purchased from Welgene (Gyeongsan, Republic of Korea). EnGen Lba Cas12a (Cpf1) was purchased from New England BioLabs (Ipswich, MA, USA). Forty percent acrylamide/bis solution (19:1) was purchased from Bio-Rad (Hercules, CA, USA). Tris−HCl (1 M; pH 7.2) was purchased from Biosesang (Seongnam, Republic of Korea). A Synergy H1 hybrid multimode microplate reader and a Cytation hybrid multimode reader (Winooski, VT, USA) were used to measure fluorescence.

2.2. Preparation of Urease-Conjugated Oligodeoxynucleotide (urODN). First, a 6.4 mM Sulfo-SMCC solution in water and 100 μM 5′-amine and 3′-biotin-modified single-stranded oligodeoxynucleotide (ssODN) solution in DEPC water were prepared. 10 μL of ssODN (1 nmol) and 7 μL of Sulfo-SMCC solution (45 nmol) were mixed and adjusted to a final reaction volume of 100 μL with 1× PBS buffer and allowed to react at 25 °C for 1 h. After reaction, the mixture was passed through a membrane-based molecular sizing centrifugal column with a molecular weight cutoff (MWCO) of 3 kDa (Merck Millipore, Billerica, MA, USA) to remove excess Sulfo-SMCC. The column was washed with 500 μL of 1× PBS buffer thrice, and maleimide-activated oligodeoxynucleotides were resuspended in 100 μL of 1× PBS buffer to a final concentration of 10 μM. And then, the maleimide-DNA was subjected to a thiol-coupling reaction with urease via the maleimide group in a slightly acidic buffer (pH 6.5). 1.5 mg of urease dispersed in 400 μL of 1× PBS solution was mixed with maleimide-activated oligodeoxynucleotides prepared in the previous step, and the conjugation reaction was allowed to proceed at 25 °C overnight. The mixture was filtered through a 100 kDa cutoff centrifugal column (Merck Millipore, Billerica, MA, USA). The urease-conjugated oligodeoxynucleotide (urODN) was then washed with 500 μL of 1× PBS buffer thrice and resuspended in 100 μL of 1× PBS to a final concentration of 10 μM.

2.3. Immobilization of urODN to Magnetic Beads (MB@urODN). First, 300 μg of magnetic bead was washed twice using 500 μL of binding and washing buffer (B&W buffer; 5 mM Tris−HCl, 0.5 mM EDTA, 1 M NaCl, 0.05% Tween 20; pH 7.5) and resuspended in 500 μL of B&W buffer. Subsequently, 100 pmol of urODN was added, followed by incubation for 2 h with gentle rotation at 1 rpm. After incubation, the urODN-immobilized magnetic beads (MB@urODN) were magnetically separated and washed thrice with 500 μL of B&W buffer and finally dispersed in 30 μL of B&W buffer. The final concentration of MB@urODN was estimated to be 10 mg/mL.

2.4. Collateral DNase Activity Using Cas12a. CRISPR/Cas12a solution was prepared by mixing equal volumes of 2 μM LbCas12a and 1 μM crispr RNA (crRNA) at 37 °C for 1 h. To confirm the collateral DNase activity of Cas12a based on fluorescence, reaction solution was prepared as 50 μL of solution containing 10 μL of various concentrations of target, 2 μL of reporter probe F-ssDNA-Q (50 μM), 10 μL of Cas12a/crRNA (0.5 μM), 5 μL of 10× NEB 2.1 buffer, and 23 μL of DEPC-treated water. Subsequently, the fluorescence intensity of the solution was measured using a hybrid

https://doi.org/10.1021/acssensors.2c02007
ACS Sens. 2022, 7, 3940−3946

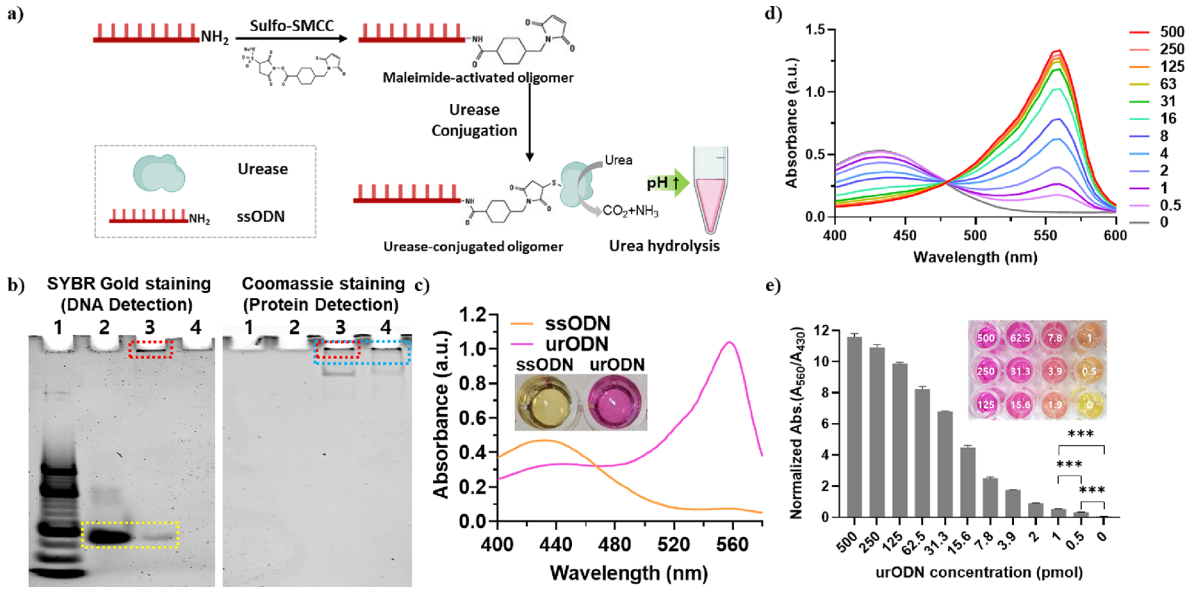

Figure 2. Synthesis and characterization of urease-conjugated single-stranded oligodeoxynucleotide (urODN). (a) Principle of cross-linking single-stranded oligodeoxynucleotide (ssODN) with urease. (b) Analysis of the conjugation of ssODN to urease using non-denaturing polyacrylamide gel electrophoresis. (c) UV−vis absorption spectra of the substrate solutions with non-modified ssODN and urODN. Inset: corresponding photograph of the substrate solutions. (d) Absorption spectrum according to urODN concentration. (e) The ratio of absorption intensity at 560 nm versus at 430 nm of the substrate solutions with different urODN concentrations after 30 min of reaction. Inset: the corresponding photograph of the substrate solutions [illustration created with BioRender.com].

multimode microplate reader (Winooski, VT, USA). The excitation wavelength was 480 nm, and the emission was monitored at 520 nm. For a colorimetric-based assay using MB@urODN, reaction solution was prepared as 50 μL of solution containing 5 μL of various concentrations of target, 30 μL of MB@urODN (10 mg/mL), 10 μL of Cas12a/crRNA (0.5 μM), and 5 μL of 10× NEB 2.1 buffer and incubated for 30 min at 37 °C. Following magnetic separation, 40 μL of the supernatant was transferred into a 96-well microplate, followed by the addition of 130 μL of substrate solution, 10 μL of 1× PBS, 130 μL of urea substrate solution (2 M NaCl, 60 mM $MgCl_2$, 50 mM urea, 1 mM HCl), and 0.04% phenol red.

2.5. Porcine Biological Sample Preparation. DNA was extracted from clinical tissue samples, including the spleen and kidney, using a DNeasy Blood & Tissue Kit, QIAGEN GmbH (Hilden, Germany), according to the manufacturer's instructions (Mai et al. 2021). In brief, the clinical samples were incubated with 180 μL of lysis buffer containing 20 μL of proteinase K, vortexed, and incubated at 56 °C until the complete lysis. Further, DNA was eluted by adding 100 μL of nuclease-free water and stored at −80 °C until further analysis.

The identification of positive and negative samples of ASFV in DNA was performed by real-time PCR using an ASFV-specific detection kit, VDx ASFV gene diagnosis (Chuncheon-si, Republic of Korea). Clinical samples for ASF detection were collected from pigs that had died due to ASF in Vietnam without capture. The ethical approval was waived as no live animals were used in this study.

3. RESULTS AND DISCUSSION

3.1. Feasibility of Urease-Conjugated Single-Stranded Oligodeoxynucleotide (urODN). The single-stranded oligodeoxynucleotide (ssODN) modified with 5′-amine and 3′-biotin was successfully conjugated to the cysteine in the urease via the heterobifunctional cross-linker (Figure 2a). The ssODN was first allowed to react with Sulfo-SMCC, resulting in maleimide-activated ssODN, followed by the coupling of urease by adding thiol to the double bond of maleimide. Using polyacrylamide gel electrophoresis, we showed that urease had successfully bound to the 5-terminal of ssODN (urODN) (Figure 2b). Lane 1 has a 10 bp DNA ladder, and lanes 2 through 4 are samples ssODN, urODN, and urease, respectively. The gel was stained with SYBR gold for gene detection, bands marked with a yellow box indicate ssODN, and it is presumed to be a urease-conjugated ssODN because of the band marked with a red box did not pass through the gel. Moreover, to confirm the presence of urease, the gel was stained with Coomassie blue, which binds only to the proteins. No bands were observed in lanes 1 and 2, and bands marked with a blue box were observed in lanes 3 and 4, confirming the presence of urease (Figure 2b). The band marked under the red box was detected under both DNA and protein staining, thereby suggesting the presence of the final product urODN at the top of lane 3.

In a subsequent procedure, absorbance was measured to confirm the binding between urease and ssODN. In the presence of urease, ammonia is produced, which changes the pH and the solution's color, shifting the absorption spectrum from 430 to 560 nm (Figure 2c). Moreover, the dramatic change in the color of the solution from yellow to magenta in the presence of urease is also shown in the photograph provided.

Following that, the absorbance was measured to evaluate whether the activity has changed depending upon the concentration of urODN (Figure 2d). The absorption spectrum changed based on the concentration of urODN, wherein a clear peak at 560 nm was observed from 500 to 0.5 pmol. For accurate comparison, the ratio of absorption intensity at 560 nm to absorption intensity at 430 m (A_{560}/A_{430}) was chosen. As shown in Figure 2e, the A_{560}/A_{430} values were obtained at 0.34 for the 0.5 pmol column and 0.07 for the 0 pmol column, showing an approximate 4.74-fold difference between the two concentrations. Therefore, colorimetric change analysis using urease was found to be applicable.

3.2. Fabrication of urODN-Immobilized Magnetic Beads (MB@urODN). We synthesized particles with varying

https://doi.org/10.1021/acssensors.2c02007
ACS Sens. 2022, 7, 3940−3946

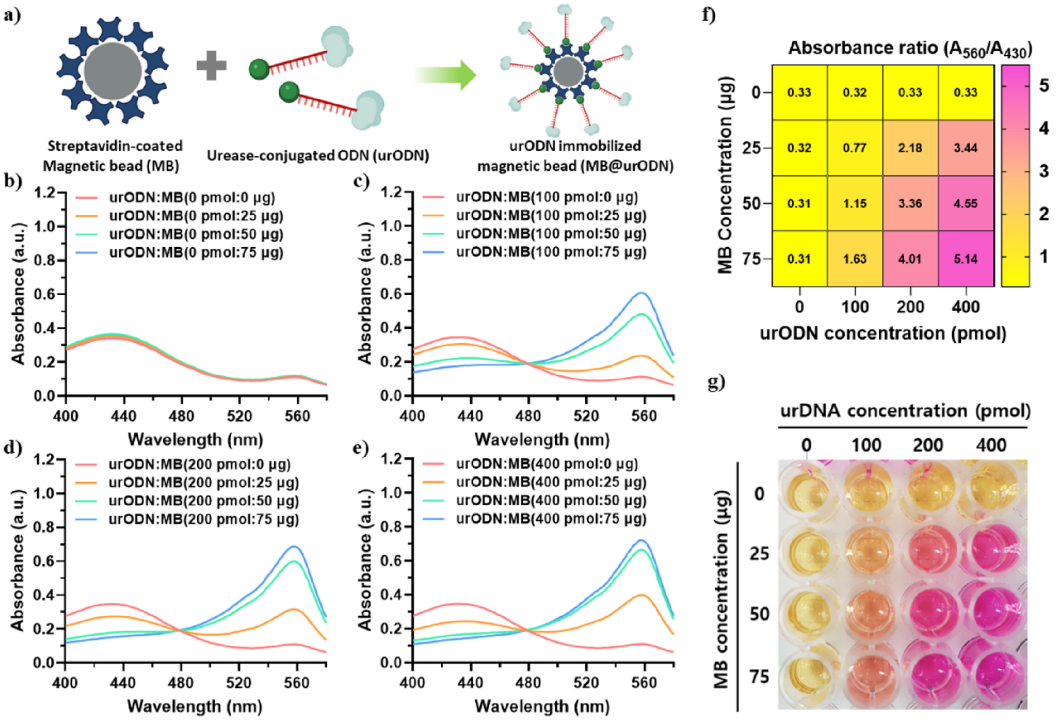

Figure 3. Characterization of the urODN-immobilized magnetic beads (MB@urODN). (a) Schematic of the synthesis of MB@urODN. (b–e) Absorption spectra of MB@urODN with different concentration ratios of magnetic beads (MBs) and urODN. (f) Heat map graph of the ratio of absorption intensity at 560 to 430 nm of substrate solutions under different conditions and (g) corresponding photograph [illustration created with BioRender.com].

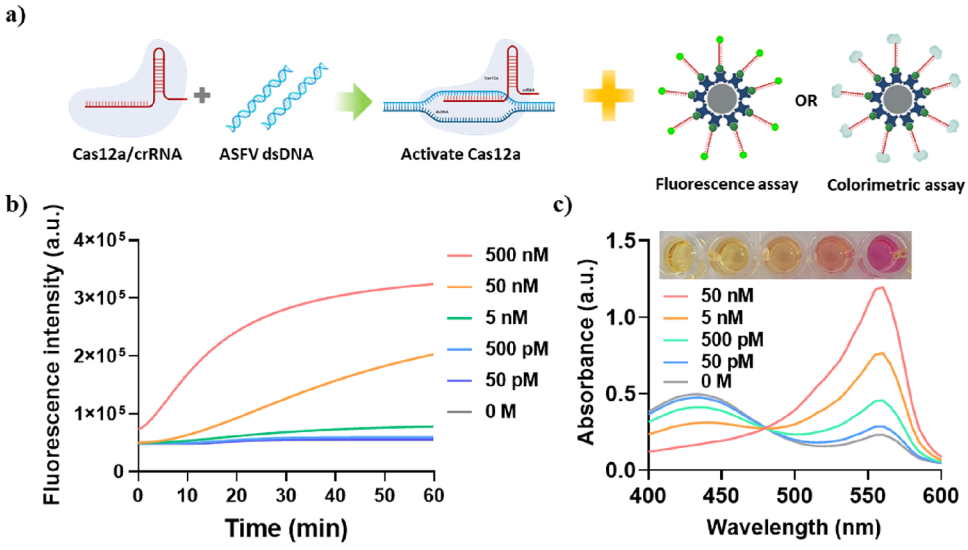

Figure 4. Design and validation of the CRISPR–Cas12a assay for ASFV dsDNA. (a) Schematic of the CRISPR–Cas12a-based assay. (b) Fluorescence kinetics measurements and the comparison of fluorescence amplification capability for the detection of ASFV dsDNA by the CRISPR–Cas12a assay with diluted target concentration using a FAM-conjugated single-stranded ODN probe. (c) Absorbance graph with various concentrations of ASFV dsDNA and corresponding photograph [illustration created with BioRender.com].

ratios of magnetic bead (MB) and urease-conjugated oligodeoxynucleotide (urODN) and validated their hydrolytic capacity to create urODN-immobilized magnetic beads (MB@urODN) that performed well for this sensing platform. Through avidin–biotin interactions, the 3′-end of the urODN was biotinylated and immobilized on a streptavidin-coated MB (Figure 3a). The absorption peak of the substrate in the absence of urODNs appeared at 430 nm, as shown in Figure 3b, and no shift was obtained based on the MB content. However, the hydrolytic effect of urease was maintained even when it was immobilized on the surface of MBs (Figure 3c–e). The absorption spectra showed that the amount of urODN anchored to the MB surface increased with the increase in the concentration of urODN. Moreover, at the absorbance ratio of 560 to 430 nm of one or more, the color of the substrate solution changed to bright orange; at the ratio of two or more, the color of the reaction solution changed more conspicuously to coral color (Figure 3f). Under the absorbance ratio of 560 to

https://doi.org/10.1021/acssensors.2c02007
ACS Sens. 2022, 7, 3940–3946

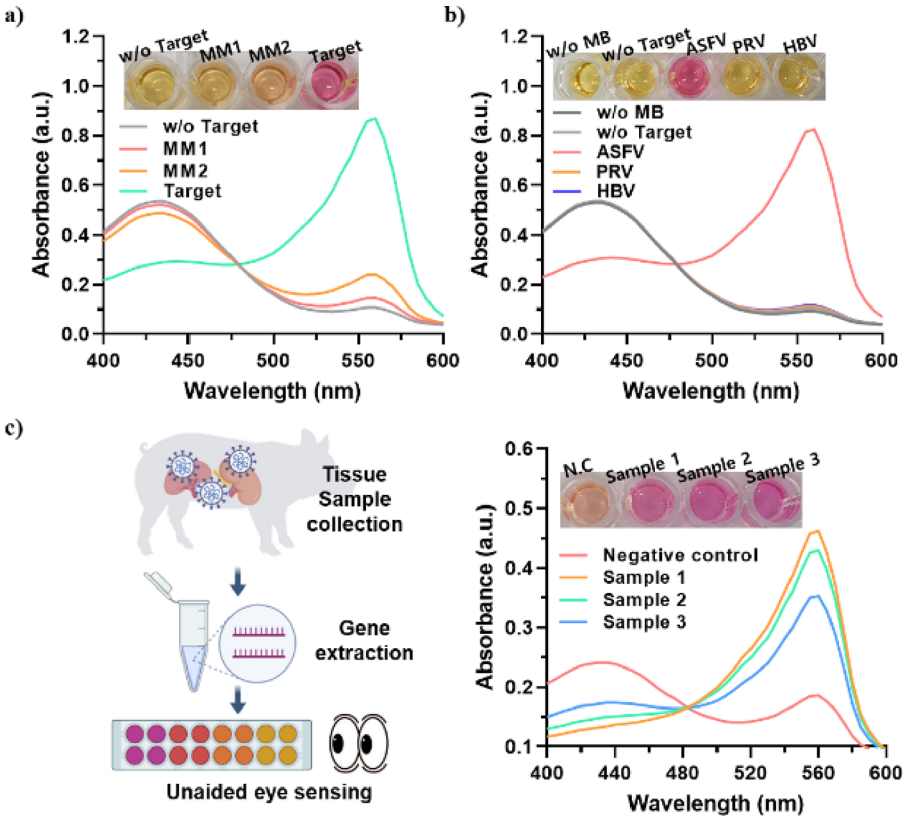

Figure 5. (a) Variation of the absorbance intensity in the presence of the target ASFV dsDNA and other 1-base mismatch targets. (b) Absorption spectrum of viruses with similar clinical symptoms. (c) Absorption spectrum applied to clinical samples taken from the porcine tissue samples [illustration created with BioRender.com].

430 nm of three or more, the color changed abruptly from yellow to magenta, as shown in Figure 3g.

3.3. Feasibility of DNase Activity of Cas12a Guided by crRNA. For ASFV detection, cleavage efficiency, detection sensitivity, an appropriate target DNA site, and crRNA were evaluated based on the protocols used in a previous study.[25] Subsequently, we confirmed the *trans*-cleavage activity of the CRISPR/Cas12a system in the presence of target DNA, wherein upon introduction target DNA hybridized with crRNA to trigger the *trans*-cleavage activity of the CRISPR/Cas12a system and activated Cas12a nonspecifically cleaved ssODN. Depending on the type of ssODN used, its presence can be measured using fluorescence- or colorimetric-based platforms (Figure 4a).

First, to evaluate the DNase activity of Cas12a, ssODN harboring a fluorophore at the 5′-end and a biotin at the 3′-end (FAM-ssODN) were used. Samples with different concentrations of the target (500, 50, and 5 nM, 500, 50, and 0 pM) were analyzed using a fluorescence assay (Figure 4b). The fluorescence intensity obtained from the reaction kinetics indicated that the concentration of the dsDNA target, the *trans*-cleavage activity of Cas12a, and the fluorescence intensity were positively correlated. The fluorescence graph demonstrated a correlation between the concentration of the dsDNA target and the *trans*-cleavage activity of Cas12a. Moreover, the group with the 50 pM dsDNA target exhibited a significant difference in fluorescence intensity compared to the blank group, thereby highlighting the high detection sensitivity of this method at as lower concentration as 50 pM, without any need for the DNA amplification process.

In a subsequent procedure, an identical sensitivity test was performed using MB@urODN, and the results were evaluated using absorption spectrum analysis and observed by naked eyes. The visual assay for urease was comprised of two components of the Cas12a *trans*-cleavage system, and a visible signal readout was based on hydrolytic degradation. The collateral DNase activity of CRISPR/Cas12a was triggered in the presence of target DNA, and urease was released from conjugated MBs, upon ssODN linker cleavage by activated Cas12a. Following the removal of residual MB@urODN by magnetic separation, the urease released in the supernatant was subjected to a cascade reaction to initiate the catalysis of urea hydrolysis. As shown in Figure 4c, the urease released from MB induced a color change in the solution due to the DNase activity of Cas12a, and this platform validated the sensitivity by one order of magnitude lower than that achieved using the fluorescent probe. The urease released from MB induced a color change in the solution.

3.4. Specificity and Sensitivity of the ASFV Sensing Platform Using Biological Samples. An experiment was performed to confirm that the sensing platform presented in this study can be applied to POCT using a DNA sample collected from porcine clinical tissue samples (Figure 5). The sensing system was challenged with multiple dsDNA targets as a perfect match with ASFV and two types of 1-base mismatch ASFV dsDNA to validate the selectivity of the MB@urODN-based colorimetric sensing platform. Figure 5a shows that the absorbance peak shift in the presence of dsDNA ASFV was 5.95 and 3.61 times greater than that of mismatched-target-1 (MM1) and mismatched-target-2 (MM2), respectively. Moreover, the POCT sensor must confer the specificity to detect

https://doi.org/10.1021/acssensors.2c02007
ACS Sens. 2022, 7, 3940−3946

only the target disease and not react with the DNAs of other diseases. Pseudorabies virus (PRV) and hepatitis B virus (HBV) possess the same dsDNA gene as ASFV, and their infections are characterized by clinical symptoms similar to ASF. An experiment was conducted to confirm the ability of the sensor to specifically detect ASFV among other disease groups (Figure 5b). The absorbance intensity at 560 nm in the presence of ASFV was observed as 8.21 and 7.81 times higher than that of the PRV and HBV, respectively, as shown in the absorbance spectra and photographs. Furthermore, an experiment was carried out to detect ASFV in porcine clinical samples (Figure 5c). The absorbance at 560 nm of three porcine samples collected was 2.48-, 2.31-, and 1.89-fold higher than the negative control, further validating the applicability and potential of the sensor under clinical settings.

4. CONCLUSIONS

The socioeconomic impacts of zoonotic and non-zoonotic diseases can be severe and widespread; hence, it is essential to diagnose the disease rapidly to monitor and prevent its spread. In countries with poor farm settings, it is crucial to implement a method for disease monitoring that omits the need for expensive and complex measurement or instrumentation. We proposed a visible, rapid, and simple nucleic acid detection approach in this study, which provides a promising platform for the early diagnosis of infectious diseases. Our colorimetric sensing platform based on the MB@urODN and CRISPR/Cas12a system provides several advantages over conventional DNA detection methods, such as the following: (i) CRISPR/Cas12a specifically recognizes the target, cleaves single-stranded oligodeoxynucleotides, and liberates urease from magnetic beads. (ii) Urease-mediated colorimetric readout with the increased signal-to-noise ratio. It has great potential applications in resource-limited farms and developing countries as it does not require thermostats or other extensive measuring equipment.

■ ASSOCIATED CONTENT

Supporting Information

The Supporting Information is available free of charge at https://pubs.acs.org/doi/10.1021/acssensors.2c02007.

Additional information on the sequence information of the oligomers used in this experiment and the summary of portable nucleic acid detection systems (PDF)

■ AUTHOR INFORMATION

Corresponding Authors

Tae Geol Lee − *Center for Nano-Bio Measurement, Korea Research Institute of Standards and Science (KRISS), Daejeon 34113, Republic of Korea; Department of Nano Science, University of Science and Technology (UST), Daejeon 34113, Republic of Korea;* orcid.org/0000-0002-6674-4147; Email: tglee@kriss.re.kr

Eun-Kyung Lim − *Bionanotechnology Research Center, Korea Research Institute of Bioscience and Biotechnology (KRIBB), Daejeon 34141, Republic of Korea; Department of Nanobiotechnology, KRIBB School of Biotechnology, University of Science and Technology (UST), Daejeon 34113, Republic of Korea; School of Pharmacy, Sungkyunkwan University, Suwon 16419, Republic of Korea;* orcid.org/0000-0003-2793-3700; Phone: +82-42-879-8456; Email: eklim1112@kribb.re.kr

Authors

Jisun Ki − *Bionanotechnology Research Center, Korea Research Institute of Bioscience and Biotechnology (KRIBB), Daejeon 34141, Republic of Korea*

Hee-Kyung Na − *Center for Nano-Bio Measurement, Korea Research Institute of Standards and Science (KRISS), Daejeon 34113, Republic of Korea;* orcid.org/0000-0001-9925-1149

Sun Woo Yoon − *Department of Biological Sciences and Biotechnology, Andong National University, Andong 36729, Republic of Korea*

Van Phan Le − *Department of Microbiology and Infectious Disease, College of Veterinary Medicine, Vietnam National University of Agriculture, Hanoi 100000, Vietnam*

Complete contact information is available at: https://pubs.acs.org/10.1021/acssensors.2c02007

Author Contributions

J.K. conceived the initial concept and designed the experiments. J.K., S.W.Y., and V.P.L. executed the experiments. H.-K.N. analyzed the data. J.K. and E.-K.L wrote the manuscript. J.K., T.G.L., and E.-K.L. edited and discussed the manuscript, and all authors approved the whole paper.

Notes

The authors declare no competing financial interest.

■ ACKNOWLEDGMENTS

This research was supported and funded by National R&D Programs through the National Research Foundation (NRF) of Korea, funded by the Ministry of Science and ICT (MSIT) of Korea (NRF-2018M3D1A1058814, NRF-2021M3E5E3080379, NRF-2018M3A9E2022821, and NRF-2022R1C1C1008815), Korea Evaluation Institute of Industrial Technology (KEIT) grant, Korean government (MOTIE) (no. RS-2022-00154853), the Technology Development Program for Biological Hazards Management in Indoor Air through the Korea Environment Industry & Technology Institute (KEITI), Ministry of Environment (ME) of Korea (2021003370003), and the KRIBB Research Initiative Program (1711134081).

■ ABBREVIATIONS

ASFV, African swine fever virus; CRISPR, clustered regularly interspaced short palindromic repeats; Cas12a, CRISPR-associated protein 12a; MB@urODN, magnetic bead-anchored urease-conjugated single-stranded oligodeoxynucleotide; PRV, pseudorabies virus; HBV, hepatitis B virus; urODN, urease-conjugated single-stranded oligodeoxynucleotide; ssODN, single-stranded oligodeoxynucleotide; dsDNA, double-stranded DNA

■ REFERENCES

(1) Eustace Montgomery, R. On A Form of Swine Fever Occurring in British East Africa (Kenya Colony). *J. Comp. Pathol. Ther.* **1921**, *34*, 159−191.

(2) Mason-D'Croz, D.; Bogard, J. R.; Herrero, M.; Robinson, S.; Sulser, T. B.; Wiebe, K.; Willenbockel, D.; Godfray, H. C. J. Modelling the global economic consequences of a major African swine fever outbreak in China. *Nat. Food* **2020**, *1*, 221−228.

(3) Dolores Gavier-Widén, K. S.; Dixon, L. No hasty solutions for African swine fever. *Science* **2020**, *367*, 622.

(4) Galindo, I.; Alonso, C. African Swine Fever Virus: A Review. *Viruses* **2017**, *9*, 107.

(5) Ma, J.; Chen, H.; Gao, X.; Xiao, J.; Wang, H. African swine fever emerging in China: Distribution characteristics and high-risk areas. *Prev. Vet. Med.* **2020**, *175*, No. 104861.
(6) Capo, A.; Calabrese, A.; Frant, M.; Walczak, M.; Szczotka-Bochniarz, A.; Manessis, G.; Bossis, I.; Staiano, M.; D'Auria, S.; Varriale, A. SPR-Based Detection of ASF Virus in Cells. *Int. J. Mol. Sci.* **2022**, *23*, 7463.
(7) James, H. E.; et al. Detection of African swine fever virus by loop-mediated isothermal amplification. *J. Virol. Methods* **2010**, *164*, 68−74.
(8) Taylor, S. C.; Nadeau, K.; Abbasi, M.; Lachance, C.; Nguyen, M.; Fenrich, J. The Ultimate qPCR Experiment: Producing Publication Quality, Reproducible Data the First Time. *Trends Biotechnol.* **2019**, *37*, 761−774.
(9) Ludwig, K. U.; et al. LAMP-Seq enables sensitive, multiplexed COVID-19 diagnostics using molecular barcoding. *Nat. Biotechnol.* **2021**, *39*, 1556−1562.
(10) Tomita, N.; Mori, Y.; Kanda, H.; Notomi, T. Loop-mediated isothermal amplification (LAMP) of gene sequences and simple visual detection of products. *Nat. Protoc.* **2008**, *3*, 877−882.
(11) Lobato, I. M.; O'Sullivan, C. K. Recombinase polymerase amplification: Basics, applications and recent advances. *Trends Analyt. Chem.* **2018**, *98*, 19−35.
(12) Piepenburg, O.; Williams, C. H.; Stemple, D. L.; Armes, N. A. DNA detection using recombination proteins. *PLoS Biol.* **2006**, *4*, No. e204.
(13) Reid, M. S.; Le, X. C.; Zhang, H. Exponential Isothermal Amplification of Nucleic Acids and Assays for Proteins, Cells, Small Molecules, and Enzyme Activities: An EXPAR Example. *Angew. Chem., Int. Ed.* **2018**, *57*, 11856−11866.
(14) Özay, B.; McCalla, S. E. A review of reaction enhancement strategies for isothermal nucleic acid amplification reactions. *Sens. Actuators Rep.* **2021**, 3.
(15) Hobbs, E. C.; Colling, A.; Gurung, R. B.; Allen, J. The potential of diagnostic point-of-care tests (POCTs) for infectious and zoonotic animal diseases in developing countries: Technical, regulatory and sociocultural considerations. *Transbound Emerg. Dis.* **2021**, *68*, 1835−1849.
(16) Rolando, J. C.; Jue, E.; Barlow, J. T.; Ismagilov, R. F. Real-time kinetics and high-resolution melt curves in single-molecule digital LAMP to differentiate and study specific and non-specific amplification. *Nucleic Acids Res.* **2020**, *48*, No. e42.
(17) Tian, B.; Minero, G. A. S.; Fock, J.; Dufva, M.; Hansen, M. F. CRISPR-Cas12a based internal negative control for nonspecific products of exponential rolling circle amplification. *Nucleic Acids Res.* **2020**, *48*, e30.
(18) Liang, M.; et al. A CRISPR-Cas12a-derived biosensing platform for the highly sensitive detection of diverse small molecules. *Nat. Commun.* **2019**, *10*, 3672.
(19) Mao, Z.; et al. CRISPR/Cas12a-based technology: A powerful tool for biosensing in food safety. *Trends Food Sci. Technol.* **2022**, *122*, 211−222.
(20) Kim, H.; et al. Enhancement of target specificity of CRISPR-Cas12a by using a chimeric DNA-RNA guide. *Nucleic Acids Res.* **2020**, *48*, 8601−8616.
(21) Gootenberg, J. S.; et al. Nucleic acid detection with CRISPR-Cas13a/C2c2. *Science* **2017**, *356*, 438−442.
(22) Li, S. Y.; Cheng, Q. X.; Wang, J. M.; Li, X. Y.; Zhang, Z. L.; Gao, S.; Cao, R. B.; Zhao, G. P.; Wang, J. CRISPR-Cas12a-assisted nucleic acid detection. *Cell Discov.* **2018**, *4*, 20.
(23) Mustafa, M. I.; Makhawi, A. M. SHERLOCK and DETECTR: CRISPR-Cas Systems as Potential Rapid Diagnostic Tools for Emerging Infectious Diseases. *J. Clin. Microbiol.* **2021**, *59*, e00745−e00720.
(24) Choi, J.-H.; Lim, J.; Shin, M.; Paek, S.-H.; Choi, J.-W. CRISPR-Cas12a-Based Nucleic Acid Amplification-Free DNA Biosensor via Au Nanoparticle-Assisted Metal-Enhanced Fluorescence and Colorimetric Analysis. *Nano Lett.* **2021**, *21*, 693−699.
(25) Lu, S.; Li, F.; Chen, Q.; Wu, J.; Duan, J.; Lei, X.; Zhang, Y.; Zhao, D.; Bu, Z.; Yin, H. Rapid detection of African swine fever virus using Cas12a-based portable paper diagnostics. *Cell Discov.* **2020**, *6*, 18.

https://doi.org/10.1021/acssensors.2c02007
ACS Sens. 2022, 7, 3940−3946